Multiscale complexity of correlated Gaussians

Richard Metzler
New England Complex Systems Institute, 24 Mt. Auburn Street, Cambridge, Massachusetts 02138, USA and Department of Physics, Massachusetts Institute of Technology, Cambridge, Massachusetts 02139, USA

Yaneer Bar-Yam
New England Complex Systems Institute, 24 Mt. Auburn Street, Cambridge, Massachusetts 02138, USA
(Received 17 December 2004; published 13 April 2005)

We apply a recently developed measure of multiscale complexity to the Gaussian model consisting of continuous spins with bilinear interactions for a variety of interaction matrix structures. We find two universal behaviors of the complexity profile. For systems with variables that are not frustrated, an exponential decay of multiscale complexity in the disordered regime shows the presence of small-scale fluctuations and a logarithmically diverging profile of fixed shape near the critical point describes the spectrum of collective modes. For frustrated variables, oscillations in complexity indicate the presence of global or local constraints. These observations show that the multiscale complexity may be a useful tool for interpreting the underlying structure of systems for which pair correlations can be measured.

DOI: 10.1103/PhysRevE.71.046114 PACS number(s): 05.70.−a, 89.70.+c, 64.60.Cn

I. INTRODUCTION

With the rising interest in complex systems comes a desire to quantify how complex a given system is. Tools that may be used come from information theory [1–3] and statistical physics [4,5]. They address questions about how long a complete microscopic description of a system must be, given its constituents and constraints. However, the microscopic information (the entropy) of a system does not correspond well with intuitive concepts of complexity—a system with maximal entropy is merely random, whereas a system with minimal entropy is strongly ordered; systems commonly considered complex, on the other hand, have rich internal structure: i.e., constraints and correlations.

This problem may be resolved by the recent approach of considering the complexity on different scales [6–10]: random systems have high information content on small scales; however, microscopic degrees of freedom average out over larger scales, leading to a satisfying description in terms of a small number of variables such as volume, pressure, and temperature. Highly constrained systems, on the other hand, have roughly the same information content on all length scales. E.g., one can describe a system of many strongly bound particles by the location, orientation, and movement of the center of gravity; given the (constant) positions of the particles relative to each other, these few variables then determine everything there is to know down to microscopic scales. In contrast, truly complex systems have intermediate levels of organization. For example, a human being has interesting behaviors on a macroscopic level (the length scale of meters), which arises from the level of organs (centimeters), which are composed of cells (micrometers), which consist of biomolecules (nanometers).

A recently developed formalism [7] allows us to calculate the complexity on different levels of observation from the underlying probability distribution of the degrees of freedom of the system, which implicitly contains the interactions and constraints of the system. The purpose of this paper is to apply this formalism to Gaussian probability distributions with various structures of the covariance matrix, yielding insight into the workings of the formalism, as well as order-disorder transitions in systems with bilinear potentials. We have previously calculated the application of this formalism to a variety of systems composed of discrete variables, including coupled spins, subdivided systems, Markov chains, self-similar structures, Ising models undergoing phase transitions, and structures relevant to biological and social organizations [7–10]. Distinct approaches introduced by other groups have focused on discrete-variable time series [11,12].

The Gaussian distribution is also used in the statistical analysis of biological and social systems [13,14]. The entries of the correlation matrix are often extracted from experimental data. The beauty of Gaussians is that their probability distribution is completely specified by two-point correlations; however, higher correlations exist. As the paper will show, the multiscale formalism offers an opportunity of detecting subsets of variables that form coupled functional units, of testing for global or local constraints that manifest themselves in the correlation matrix, and for characterizing collective behaviors of systems.

The paper is organized as follows: Section II reviews properties of correlated Gaussian variables. Section III reviews the mathematical representation of physical degrees of freedom in the form of Gaussians. Section IV gives an overview of the multiscale complexity formalism and previous results. Section V then shows how the formalism applies to a variety of different interaction matrices. Section VI summarizes and interprets the results.

II. GAUSSIAN VARIABLES

Due to the pervasive power of the central limit theorem that gives rise to Gaussian distributions and due to their mathematical convenience, Gaussians are the default assumption for probability distributions under many circum-

stances. This paper discusses sets of n Gaussian variables, labeled x_i, with $i \in \{1,n\}$. Each has a mean of 0 and a variance of σ_i^2: $\langle x_i \rangle = 0$, $\langle x_i^2 \rangle = \sigma_i^2$. The cross correlations are given by the elements of the covariance matrix $\mathbf{R}$: $\langle x_i x_j \rangle = R_{ij}$. The joint probability distribution is then given by

$$P(\mathbf{x}) = \frac{1}{\sqrt{(2\pi)^n \text{ Det } \mathbf{R}}} \exp\left(-\frac{1}{2} \mathbf{x}^T \cdot \mathbf{R}^{-1} \cdot \mathbf{x} \right). \tag{1}$$

To calculate how much information is contained in a Gaussian variable, we use Shannon's information theory [1]; however, for convenience, we use natural units (base e) rather than bits; i.e., for on 1 degree of freedom, the definition is

$$I_x = -\int \ln[p(x)] p(x) dx. \tag{2}$$

For a single Gaussian of variance σ^2 this results in $I_x^G = [\ln(2\pi)+1]/2 + \ln(\sigma)$. For the joint distribution in Eq. (1), one can obtain

$$I_{\mathbf{x}} = \{n[\ln(2\pi) + 1] + \ln(\text{Det } \mathbf{R})\}/2. \tag{3}$$

For the trivial case of n uncorrelated Gaussians of variance σ^2, one has $\ln(\text{Det } \mathbf{R}) = 2n \ln \sigma$, so that the information is just n times that of a single variable.

III. PHYSICAL INTERPRETATION

There is a close formal analogy between Eq. (1) and the canonical distribution for continuous degrees of freedom with bilinear interactions $H = -\frac{1}{2}\Sigma_{ij} J_{ij} x_i x_j$:

$$P(\mathbf{x}) = \frac{\exp\left(\frac{\beta}{2} \sum_{i,j} J_{ij} x_i x_j \right)}{Z}, \tag{4}$$

where the partition function Z is the integral of the numerator over state space. We will consider two quite distinct interpretations of such a system: the first is an individual particle in a harmonic potential with n degrees of freedom, with J_{ii} giving the potential along the coordinate axes and J_{ij} determining the shape of the potential along the diagonals.

The second interpretation considers each degree of freedom as a spin that interacts with other spins. In the context of models for magnetic systems, this is called the "Gaussian model" [15] and has been used as an approximation to binary Ising spins. In the Gaussian model, it is usually assumed that spins in the absence of interactions follow a Gaussian distribution of variance 1 (independent of temperature), while off-diagonal interactions are weighted with a factor of β and there is no explicit self-interaction.

In this paper, for convenience, we consider the self-interaction, which serves to keep spins bounded, as a part of the interaction matrix. The relevant control parameter then becomes the ratio of the self-interaction to the interaction with other spins, rather than the temperature. We can then write the covariance matrix as $\mathbf{R} = (-\beta \mathbf{J})^{-1}$. Changing β or changing the magnitude of both the self-interaction J_{ii} and off-diagonal interaction J_{ij} only results in a rescaling of the variables: $\beta \Sigma x_i J_{ij} x_j = \Sigma x_i' J_{ij} x_j'$ with $x_i' = \sqrt{\beta} x_i$. This is a reflection of the equipartition theorem, which states that each degree of freedom corresponding to a quadratic term in the energy carries a mean energy of $k_B T/2$. As we show in Sec. III, such a rescaling only adds an additive term to the microscopic entropy and does not change the terms in the multiscale complexity for scales larger than 1. We can therefore set $\beta = 1$ and the self-interaction $J_{ii} = -1$ unless otherwise stated, whereas the interaction with neighbors is proportional to a parameter a which we vary to control the system's behavior.

In contrast to the Ising model, the Gaussian model does not have a well-defined ordered phase. Interpreting the system as a particle in a harmonic potential, we find that $\langle x_i^2 \rangle$ is finite (i.e., the system is in the disordered phase) if all eigenvalues of $\mathbf{J}$ are positive—otherwise, there is at least 1 degree of freedom with infinite negative energy—i.e., a harmonic potential of the form $E(x) = -\lambda x^2$, $\lambda > 0$. To model phase transitions more realistically in this framework, one would have to introduce quartic terms [16]; however, in this paper we will restrict ourselves to the pure Gaussian model. Interestingly, the transition to unbounded spins can happen in systems of any size and be due to the interaction of just two spins.

The harmonic potential interpretation also offers a geometric argument why the entropy is related to the determinant of the covariance matrix [Eq. (3)]: the coordinate system can be chosen such that the main axes of the equipotential ellipsoid coincide with the coordinate axes (i.e., the interaction matrix is diagonalized). This is always possible because the interaction matrix is symmetric. The quadratic degrees of freedom then decouple; the mean-square amplitude along each axis depends on the corresponding eigenvalue of the interaction matrix, and the information (which is a measure of the size of state space) is the sum of the information for the individual degrees of freedom. Specifically, it is related to the sum of the logarithms of the eigenvalues or, equivalently, the logarithm of the determinant. Some of the axes of the new coordinate system can be interpreted as aggregate variables such as the magnetization (the sum of all spins).

In diagonalized form, the susceptibility to external fields at the transition is easy to calculate. In the generic case, the smallest eigenvalue λ_1 can be linearly expanded around 0: $\lambda_1 = K(a - a_c)$. Applying a field h along the eigenvector of λ_1 then shifts the minimum of the energy H (i.e., induces an magnetization) to $h/[2K(a-a_c)]$ along this axis. The susceptibility is therefore proportional to $(a-a_c)^{-\gamma}$ with $\gamma = 1$, independent of the underlying dimensionality of the system. Different exponents can arise only if the linear expansion of λ_1 around 0 has a vanishing first derivative, which is not the case for any of the cases we study in the following.

The link between the entropy (or, equivalently, information) and $\ln \text{Det } \mathbf{R}$ has one mathematical difficulty: since Det $\mathbf{R}$ can go to 0, the entropy can diverge to negative infinity. The determinant vanishes if the rank of $\mathbf{R}$ is smaller than n; i.e., one or more columns can be expressed as linear combinations of others. In our context, this corresponds to a variable that is completely specified by a combination of others.

Generally, the determinant is a polynomial of order n in the coefficients of the matrix and the order of the zero in question determines how many redundant variables there are. The diverging entropy is not a problem for physical systems, since no physical quantity can be perfectly specified.

IV. MULTISCALE COMPLEXITY FORMALISM

A suitable measure of multiscale complexity $C_n(k)$ should fulfill several conditions. For the smallest scale, it should correspond to the microscopic entropy, which is the information contained in the joint probability distribution of all degrees of freedom. If the system is composed of distinct subsets of l variables that are coupled within the subset, but not coupled to other subsets, $C_n(k)$ should be 0 for $k>l$ and take nonvanishing values corresponding to the number of degrees of freedom otherwise. Furthermore, the multiscale complexity of a composite of independent subsystems should be the sum of subsystem complexities.

It has been shown in [7] that the following definition uniquely fulfills these conditions:

$$C_n(k) = \sum_{j=0}^{k-1} (-1)^{k-j-1} \binom{n-j-1}{k-j-1} Q(n,j), \tag{5}$$

with

$$Q(n,k) = -\sum_{\{j_1,\ldots,j_k\}} \int \prod_{i_{k+1}}^{i_n} dx_i P(\mathbf{x}-\{x_j\}) \ln P(\mathbf{x}-\{\mathbf{x}_j\}). \tag{6}$$

Equation (6) is a sum over all subsets of k variables of the entropy of the system after the subset has been removed. Thus, $Q(n,0)$ is the microscopic entropy and $Q(n,n-1)$ is the sum of entropies for individual degrees of freedom. The formalism can be applied to any system that can be described by a probability measure, equilibrium or nonequilibrium systems, or a time series described by a stochastic (e.g., Markov) process [7–10].

It is sometimes convenient to discuss the incremental difference in complexity between scales $D(k)=C(k+1)-C(k)$. While $C(k)$ represents the effective number of degrees of freedom of size k or larger, $D(k)$ represents the effective number of degrees of freedom at scale k.

The quantity defined by Eq. (5) has some additional, rather surprising, properties. In particular, it can have oscillations and take negative values even for discrete variables. These seemingly anomalous properties have been shown to reflect the structure of the system and specifically have been linked to the effect of global constraints on local variables or more generally the concept of strong emergence in Ref. [10]. We will explore the relevance of such behavior to the Gaussian model.

To simplify the discussion further, we will show first that rescaling the variables (e.g., by choosing a different inverse temperature β, as described in Sec. II) adds a term to the microscopic entropy $C_n(1)$ that only depends on n and the scaling ratio, and does not affect higher-order complexities ($k>1$). When applied to Gaussians, the terms $Q(n,k)$ are sums over the logarithm of determinants of submatrices of $\mathbf{R}$, dropping combinations of k rows and corresponding columns. Rescaling the covariance matrix by a factor f yields an additive term of $l \ln f$ to the logarithm of the determinant of a submatrix of size $l \times l$. Since there are $\binom{n}{j}$ such contributions for $Q(n,j)$, the difference between the rescaled multiscale complexity $\hat{C}_n(k)$ and the original is

$$\begin{aligned}
\hat{C}_n(k) - C_n(k) &= \sum_{j=0}^{k-1} (-1)^{k-j-1} \binom{n-j-1}{k-j-1} \binom{n}{j} (n-j) \ln f \\
&= \sum_{j=0}^{k-1} (-1)^{k-j-1} \frac{(n-j-1)!}{(k-j-1)!(n-k)!} \\
&\quad \times \frac{n!(n-j)}{j!(n-j)!} \ln f \\
&= \binom{n}{k} k \ln f \sum_{j=0}^{k-1} (-1)^{k-j-1} \binom{k-1}{j} \\
&= \begin{cases} 0 & \text{for } k>1, \\ n \ln f & \text{for } k=1. \end{cases}
\end{aligned} \tag{7}$$

The identity in the last line can be derived by expanding $[1+(-1)]^{k-1}$ using binomial coefficients.

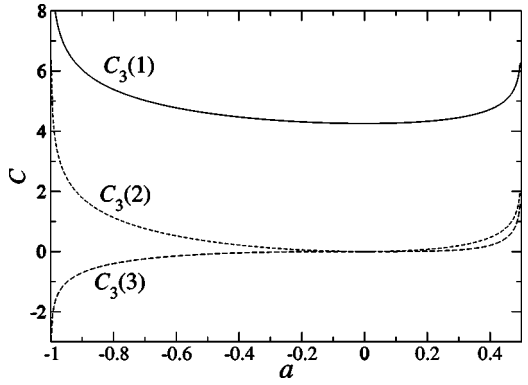

FIG. 1. Multiscale complexities for the three-spin chain. While all complexities are positive for $a>0$, $C_3(3)$ is negative for $a<0$.

V. APPLICATION TO SPECIFIC MODELS

A. Three interacting spins

We start by applying the formalism to a minimal case of three interacting spins. The three-spin case captures a number of features that will be characteristic of larger spin systems. The complexity profile can be solved analytically, giving

$$\begin{aligned}
C_3(1) &= \{3[\ln(2\pi)+1] - 2\ln(1+a) - \ln(1-2a)\}/2, \\
C_3(2) &= -\ln(1+a) - \ln(1-2a)/2, \\
C_3(3) &= [-\ln(1-2a) + \ln(1+a) + 3\ln(1-a)]/2.
\end{aligned} \tag{8}$$

As Fig. 1 shows, complexities diverge at $a=1/2$ and $a=$

-1. These are the ferromagnetic and antiferromagnetic transitions to unbounded variables. As this case illustrates, unlike conventional binary spin systems, transitions occur even for finite numbers of spins. This result can be understood by recognizing that conventional Gaussian variables themselves can be thought of as arising as aggregates of many microscopic bounded variables through the central limit theorem. Negative values of $C_3(3)$ occur for $a<0$. This is expected for systems with frustrated spins, due to the existence of a constraint on the three spins that does not affect any pair of spins.

B. Infinite-range magnet

For larger numbers of spins we consider first an infinite-range Gaussian model, with an interaction matrix

$$\mathbf{J}=\begin{pmatrix} -1 & a & \cdots & a \\ a & -1 & a & \cdots \\ a & \cdots & \cdots & a \\ a & \cdots & a & -1 \end{pmatrix}, \tag{9}$$

where a, the interaction between spins, is negative for antiferromagnets and positive for ferromagnets. Inverting the negative of this matrix does not alter its structure; one obtains the covariance matrix

$$\mathbf{R}=\begin{pmatrix} r & c & \cdots & c \\ c & r & c & \cdots \\ c & \cdots & \cdots & c \\ c & \cdots & c & r \end{pmatrix}, \tag{10}$$

with r and c given by

$$r=\frac{1-(n-2)a}{(1+a)[1-(n-1)a]}, \tag{11}$$

$$c=\frac{a}{(1+a)[1-(n-1)a]}. \tag{12}$$

We define the correlation ratio $\rho=c/r$, in order to separate the amplitude of the spins from the correlations between them:

$$\rho=\frac{a}{1-(n-2)a}. \tag{13}$$

Since ferromagnetic ordering is easier to achieve with infinite-range interactions than antiferromagnetic ordering, the transition where all spins collapse into one (ρ goes to 1) and the amplitude diverges occurs at a small value of $a=1/(n-1)$. Antiferromagnetic ordering occurs at $a=-1$, where ρ takes the asymptotic value $-1/(n-1)$ and all variables are maximally anticorrelated, taking values corresponding to an $(n-1)$-dimensional hypertetrahedron.

The determinant of $\mathbf{R}$ is

$$\mathrm{Det}\ \mathbf{R}_n=r^n(1-\rho)^{n-1}[1+(n-1)\rho]. \tag{14}$$

The determinant has a zero of order $n-1$ at $\rho=1$, where all variables are the same, and $n-1$ of them are redundant. It also has a first-order zero at $\rho_c=-1/(n-1)$, where geometrical constraints can be used to eliminate one variable.

We can now calculate the scale-dependent complexity $C_n(k)$ following Eq. (5). For our example, we can calculate this analytically for $k=1,2,3$ and numerically for other values of k. Since the matrix does not change its structure if one or more variables are removed, the determinant has the same form as Eq. (14) with a modified number of variables.

We then have

$$Q(n,j)=\binom{n}{j}\left[\frac{n-j}{2}[\ln(2\pi r)+1]+\frac{1}{2}\{(n-j-1)\ln(1-\rho)+\ln[1+(n-j-1)\rho]\}\right], \tag{15}$$

which yields

$$C_n(1)=\frac{n}{2}[\ln(2\pi)+1+\ln(r)]+\frac{n-1}{2}\ln(1-\rho)+\frac{1}{2}\ln[1+(n-1)\rho], \tag{16}$$

$$C_n(2)=\{-\ln(1-\rho)-(n-1)\ln[1+(n-1)\rho]+n\ln[1+(n-2)\rho]\}/2, \tag{17}$$

$$C_n(3)=-\ln(1-\rho)/2+(n-1)(n-2)\ln[1+(n-1)\rho]/4-n(n-2)\ln[1+(n-2)\rho]/2+n(n-1)\times\ln[1+(n-3)\rho]/4, \tag{18}$$

as shown in Fig. 2. In terms of a, these complexities can be written as

$$C_n(1)=\frac{n}{2}\{\ln(2\pi)+1+\ln[1-(n-1)a]\}+\frac{n-1}{2}\times\ln[1-(n-1)a]+\frac{1}{2}\ln(1+a), \tag{19}$$

$$C_n(2)=[-\ln(1-(n-1)a)-(n-1)\ln(1+a)]/2, \tag{20}$$

$$C_n(3)=\{-2\ln[1-(n-1)a]+(n-1)(n-2)\ln(1+a)+n(n-1)\ln(1-a)\}/4. \tag{21}$$

For $n=3$ this reduces to the case of three interacting spins, Eq. (8). All complexities for $k>1$ include a singular term $-\ln(1-\rho)/2=-\ln[1-(n-1)a]/2$ but are independent of r, which is a consequence of the invariance to multiplying all spins by the same factor, as described above. $C_n(1)$, on the other hand, includes a term $\ln(2\pi r)+1$ (see Fig. 2).

We find two characteristic behaviors for ferromagnetic and antiferromagnetic interactions. In the ferromagnetic case ($a>0,\rho>0$) the multiscale complexity is positive and decreases monotonically with increasing k. The curves of $C_n(k)$ plotted as a function of k/n approximately collapse to one curve for each value of $\rho>0$, so that the complexity can be written as a scaling function $C(k/n,\rho)$. Near $\rho=1$, this function takes a universal shape, so that $C(k/n,\rho)\approx C_l(k/n)$

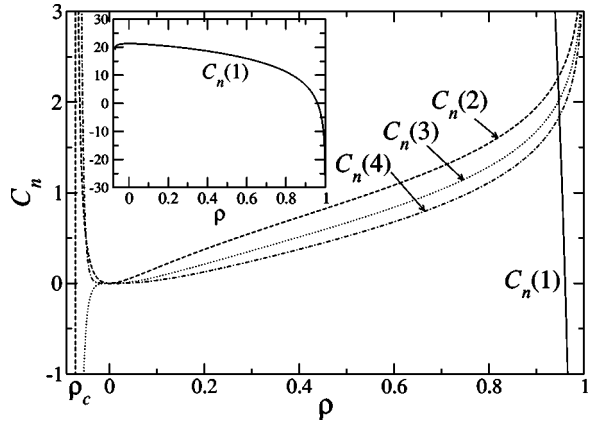

FIG. 2. Complexities $C_n(1)-C_n(4)$ for infinite-range interactions (for $n=15$ and amplitude $r=1$) following Eqs. (16)–(18). The inset shows $C_n(1)$ for a different scaling of the y axis.

$+E(\rho)$. The singular term in all complexities pointed out above, $-\ln(1-\rho)/2$, can be identified with $E(\rho)$. As seen in Fig. 3, reducing $1-\rho=\rho_c-\rho$ [or equivalently a_c-a, as seen in Eqs. (19)–(21)] by a factor of 10 increases $C_n(k/n)$ by $\ln(10)/2$.

The universal shape of $C(k/n,\rho)$ implies that $D(k)$, the spectrum of excitations, is independent of ρ near the transition. With increasing coherence of the variables, the collective behavior at $C(n)$ increases at the expense of the independence of the variables $C(1)$ without affecting the spectrum of intermediate scale excitations.

In the antiferromagnetic case ($a<0, \rho<0$) oscillations in $C_k(n)$ are found, as seen in Fig. 4. The amplitude of oscillations increases as $-f\ln[1+(n-1)\rho]-g$, where f and g increase rapidly with n and are of order 10^5 for $n=20$. Oscillatory behavior in the multiscale complexity has been linked to global constraints [10]; in this case, it is the constraint $\Sigma x_i=0$ which is enforced by the interactions near the transition point and which can be used to eliminate one of the variables.

It should be pointed out that Eq. (5) is susceptible to numerical inaccuracies, and with insufficient precision one observes oscillations for $\rho>0$; however, these are numerical

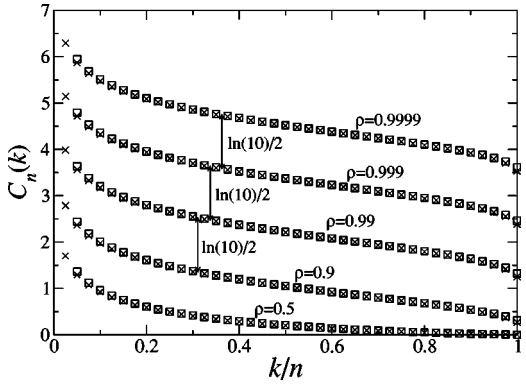

FIG. 3. Complexities $C_n(k)$ for $n=40$ (squares) and $n=80$ (crosses) for the infinite-range ferromagnet, displayed as a function of k/n, for various values of ρ. Arrows indicate the shift predicted by Eq. (18).

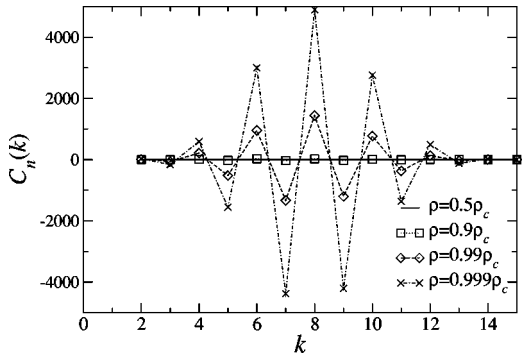

FIG. 4. Complexities $C_n(k)$ for the infinite-range antiferromagnet with $n=15$, for different values of $\rho<0$, expressed as fractions of $\rho_c=-1/(n-1)$. This is close to the point where one variable becomes redundant; the multiscale complexity shows oscillations of increasing amplitude.

artifacts, as can be seen by increasing the accuracy of calculations. The oscillations in the antiferromagnetic regime are not artifacts.

C. One-dimensional spin chain

We consider a chain of n spins with nearest-neighbor interactions a and self-interactions -1. The interaction matrix is given by

$$\mathbf{J}=\begin{pmatrix} -1 & a & 0 & \cdots & a \\ a & -1 & a & 0 & \cdots \\ & & \cdots & & \\ a & 0 & \cdots & a & -1 \end{pmatrix}. \tag{22}$$

For even n, it is not relevant whether interactions are ferromagnetic or antiferromagnetic, since both cases can be mapped onto each other by flipping every other spin. For odd n, the asymmetry with respect to a becomes less pronounced as n increases: negative complexities are only observed for $n\leqslant 5$, and for $n>15$ the curves look largely symmetric. The following observations assume even n.

For weak interactions, one finds correlations that decrease exponentially with distance; specifically, the leading-order term of R_{ij} is $a^{|i-j|}$. Due to the short-ranged, one-dimensional interactions, Ising spins with this interaction structure do not show an order-disorder phase transition. However, the continuous-spin system displays a transition from finite to infinite variances for $a=\pm 1/2$, at which point the nearest-neighbor interactions override the self-interaction.

We find numerically that $C_n(k)$ is proportional to n for small $k>1$: each additional spin takes a finite amount of information to describe (see Fig. 5). This is consistent with the short-range interactions of the model.

The complexity profile for all scales (Fig. 6) behaves similarly to the infinite-range ferromagnet (Fig. 3): as a approaches a_c, the complexity profile has a universal shape $C_n^0(k)$ that is monotonically decreasing and spans all scales. The divergence as a function of $a-a_c$ follows $C_n(k,a)=C_n^0(k)-\ln(a_c-a)$.

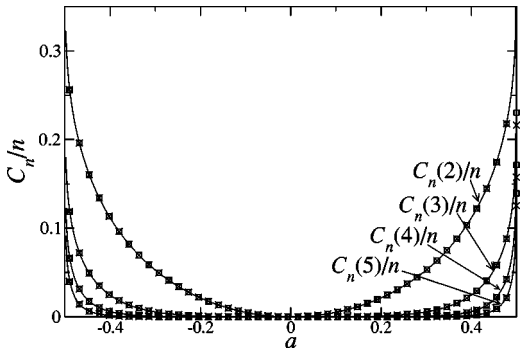

FIG. 5. Multiscale complexities for the multispin chain, normalized by the number of spins, n, for $n=16$ (lines), $n=25$ (squares), and $n=32$ (crosses).

D. Square lattice

For a two-dimensional example, we arrange spins on a $L\times L$ square lattice with periodic boundary conditions and nearest-neighbor interactions of strength a. The transition point to unbounded spins is at $a=\pm 1/4$. Intuitively, four interactions of strength $1/4$ are sufficient to balance the self-interaction of strength 1.

As with the spin chain we find that the multiscale complexities are roughly proportional to the number of spins in the system and are almost symmetric with respect to switching the sign of a. (see Fig. 7) For even L the symmetry is exact since a ferromagnetic square lattice can be transformed into an antiferromagnetic one by flipping spins in a checkerboard pattern. The symmetry is not exact for odd L and the deviation is largest for small values of L. For different L the values of $C(k)/N$ do not collapse as well, indicating a more significant deviation from extensivity than in the one-dimensional case.

The complexity profile shows a similar behavior to the infinite-range ferromagnet: as a approaches a_c, a complexity profile with universal shape emerges that spans all scales, and is monotonically decreasing, as seen in Fig. 8. A logarithmic divergence as a function of $a-a_c$ is found as before. The shape of the complexity profile in the limit is different from the previous scenarios; the cases will be compared below.

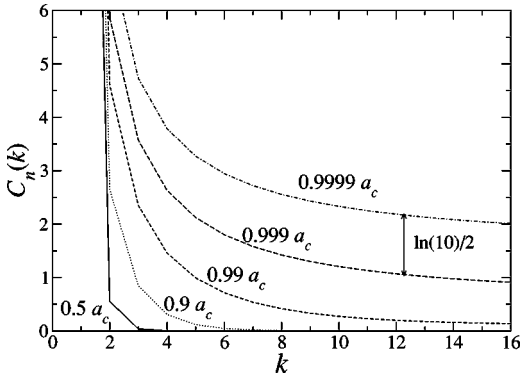

FIG. 6. Multiscale complexity for the one-dimensional spin chain with nearest-neighbor interactions, for different interaction strengths at $n=16$.

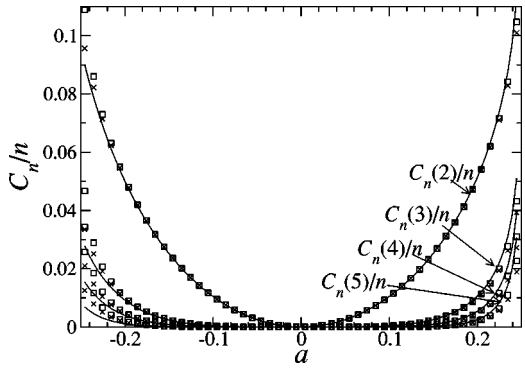

FIG. 7. Multiscale complexities for the square lattice with nearest-neighbor interactions, normalized by the number of spins, $n=L\times L$, for $L=5$ (lines), $L=6$ (squares), and $L=7$ (crosses).

E. Block matrix

We generalize the infinite-range Gaussian model by dividing the spins into groups that interact strongly within the group, but weakly with members of other groups, yielding the following interaction matrix (we explicitly label the self-interaction as $-d$ in this case):

$$\mathbf{J}=-\begin{pmatrix} d & \cdots & a & & & & & & \\ a & d & a & & b & & & b & \\ a & \cdots & d & & & & & & \\ & & & d & \cdots & a & & & \\ & b & & a & d & a & & b & \\ & & & a & \cdots & d & & & \\ & & & & & & d & \cdots & a \\ & b & & & b & & a & d & a \\ & & & & & & a & \cdots & d \end{pmatrix}, \tag{23}$$

with m blocks of n spins each. This model is important in the study of complex systems since it has a multilevel structure—i.e., modularity—considered to be a universal property of complex systems [6,17].

The determinant of this matrix is

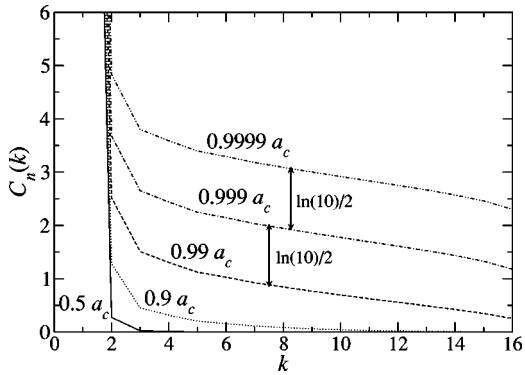

FIG. 8. Multiscale complexity for the square lattice with nearest-neighbor interactions, for different interaction strengths at $L=4$.

$$\mathrm{Det}(-\mathbf{J}) = (d-a)^{m(n-1)}[d+(n-1)a-nb]^{m-1}[d+(n-1)a + n(m-1)b], \tag{24}$$

which enables us to find the permissible ranges of d, a, and b: for bounded spins to exist, d, which is the negative self-interaction, has to be positive. Positive values of a and b imply antiferromagnetic interactions, negative ferromagnetic. The boundaries of the allowed region are given by the zeros of Eq. (24):

$$a/d \leqslant 1, \tag{25}$$

$$b/d \leqslant [1+(n-1)a/d]/n, \tag{26}$$

$$b/d \geqslant -[1+(n-1)a/d]/[n(m-1)]. \tag{27}$$

The inverse of this matrix has the same structure as Eq. (23); if we label the coefficients of $-\mathbf{J}^{-1}$ as A, B, and D, respectively, we obtain

$$D = K\{d^2+(m-2)(n-2)nab-(m-1)(n-1)nb^2 + (n-1)(n-2)a^2+[(m-2)nb+(2n-3)a]d\},$$

$$A = K[-ad-(n-1)a^2+(m-2)nab+(m-1)nb^2],$$

$$B = -K(d-a)b, \tag{28}$$

where

$$K = \{(d-a)[d+(n-1)a-nb][1+(n-1)a+(m-1)nb]\}^{-1}. \tag{29}$$

Since the inverse of the negative interaction matrix is the covariance matrix, this allows us to determine under what circumstances correlations to near and far neighbors are positive or negative. A has a zero for

$$b_{1,2} = \frac{1}{2(m-1)n}[(m-2)na \pm \sqrt{m^2n^2a^2+4(m-1)n(d-a)a}]; \tag{30}$$

it is negative between the branches of the root and positive outside. B is negative for $b<0$ and positive for $b>0$. Combining the results from Eqs. (25), (26), and (30), the phase diagram shown in Fig. 9 emerges. Interestingly, long-range interactions do not stabilize the system: at any $b\neq 0$, the system has a smaller range of stability with respect to a than for $b=0$.

We now calculate the multiscale complexities. $C_{nm}(1)$ can be calculated from the determinant, Eq. (24), with entries D, A, and B from Eq. (28):

$$C_{nm}(1) = \frac{1}{2}\{nm[\ln(2\pi)+1]+n(m-1)\ln(D-A) + (m-1)\ln[D+(n-1)A-nB] + \ln[D+(n-1)A+n(m-1)B]\}. \tag{31}$$

Unfortunately, removing spins does not leave the structure of the covariance matrix unchanged. The determinant of the matrix with one spin removed is

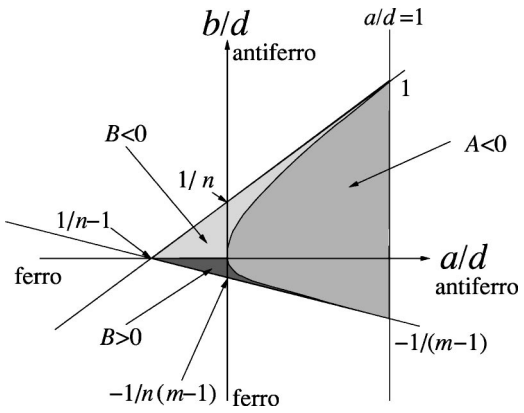

FIG. 9. Phase diagram for a block matrix with m groups of n spins each. Relevant variables are the ratios between near- and far-neighbor interactions and self-interaction. Shading indicates the sign of covariances A and B.

$$\mathrm{Det}\, C_{-1} = (D-A)^{m(n-1)-1}[D+(n-1)A-nB]^{m-2} \times\{D^2+(2n-3)AD+(n-1)(n-2)A^2+n(m-2) \times[D+(n-2)A]B-n(n-1)(m-1)B^2\}. \tag{32}$$

From this expression, the corresponding complexity for scale 2 can be found:

$$C_{nm}(2) = (1/2)(-m\ln(D-A)+(m-mn-1)\ln[D+(n-1)A - nB]-(mn-1)\ln[D+(n-1)A+n(m-1)B] + mn\ln\{D^2+(2n-3)AD+(n-1)(n-2)A^2+n(m-2)[D+(n-2)A]B-n(n-1)(m-1)B^2\}). \tag{33}$$

The first term in Eq. (33) indicates that the divergence near $A=D$ is logarithmic in $m\ln(D-A)/2$; the additional factor of m, compared to previous scenarios, indicates that there are m distinct units.

Expressions for higher k do not give additional insight. We therefore turn to numerical results, which are shown in Fig. 10. Along the $b=0$ axis, the system consists of m blocks of n coupled spins each. Complexities $C_{nm}(k)$ are different from zero for $k\leqslant n$ (positive for ferromagnetic interactions, oscillating for antiferromagnetic) and equal to zero for $k>n$. This reflects the built-in property of the multiscale formalism to identify noninteracting subsets of variables.

For $b\neq 0$, complexities at scales up to $k=nm$ become nonzero. In the quadrant $a<0, b<0$ where all interactions are ferromagnetic, all complexities are larger than zero. In the other quadrants, one observes either negative complexities for higher scales or oscillations similar to those found for the infinite-range antiferromagnet. We expect a similar picture to hold for more than two levels of hierarchy: a monotonically decreasing curve with kinks at the scales corresponding to block sizes if all interactions are ferromagnetic (as in the lower left panel of Fig. 10) and combinations of decreasing curves and oscillations on different scales if both ferromagnetic and antiferromagnetic interactions are present.

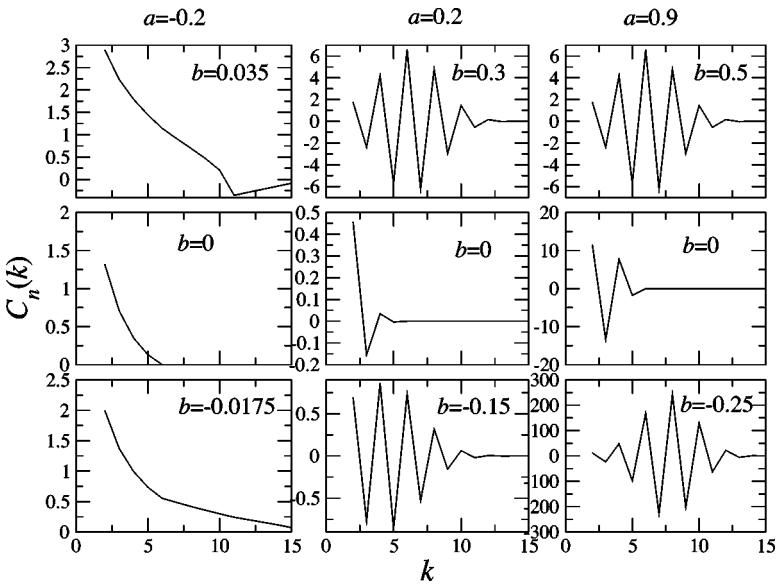

FIG. 10. Multiscale complexities for block structure interactions with $n=5$, $m=3$, for different values of a and b.

F. Infinite-range spin glass

Spin glasses (magnetic systems with random ferromagnetic or antiferromagnetic interactions) are a well-studied model of systems with frustrated interactions, multiple degenerate ground states, and other interesting features [19,20]. The multiscale complexity of spin glasses is therefore of considerable interest. We consider interaction matrices with diagonal elements $J_{ii}=-1$ and off-diagonal elements $J_{ij}=J_{ji}=ar_{ij}$, where r_{ij} is a Gaussian random variable of variance 1. To determine transition points for any one realization of the quenched random interactions, we keep the set of r_{ij} constant and adjust the interaction strength a.

The first quantity of interest is the critical a at which the transition from bounded to unbounded variances occurs. This is related to the eigenvectors of $-J$, which are necessarily all positive for bounded spins. The spectrum of eigenvalues λ of Gaussian matrices has been studied [18]; if all entries (including the diagonal) are Gaussians of mean 0 and variance σ^2, the matrix is symmetric and n is large; it takes the form

$$P(\lambda)=\begin{cases}(2\pi\sigma^2 n)^{-1}\sqrt{4\sigma^2 n-\lambda^2} & \text{for } |\lambda|<2\sigma\sqrt{n},\\ 0 & \text{else,}\end{cases} \tag{34}$$

i.e., a semicircle of a width proportional to $a\sqrt{n}$. For small n, the cutoff of this semicircle becomes blurred.

Calculations show that replacing the random diagonal elements with nonrandom elements of magnitude d has two effects: n is replaced by $n-1$ in Eq. (34), and the mean of the distribution is shifted by d (as can be shown analytically). Thus, the distribution of λ follows $P(\lambda)=\sqrt{4\sigma^2(n-1)-(\lambda-d)^2}/[2\pi\sigma^2(n-1)]$.

The critical interaction value a_c is that for which the smallest eigenvalue becomes 0 for $d=1$. Neglecting the blurring of boundaries, we thus expect $|a_c|=d/\sqrt{4(n-1)}$, which is in good agreement with calculations for large n. It should be pointed out that a_c has significant fluctuations for small n—the exact transition point differs for each realization of $\{r_{ij}\}$. These result indicate a significant difference in

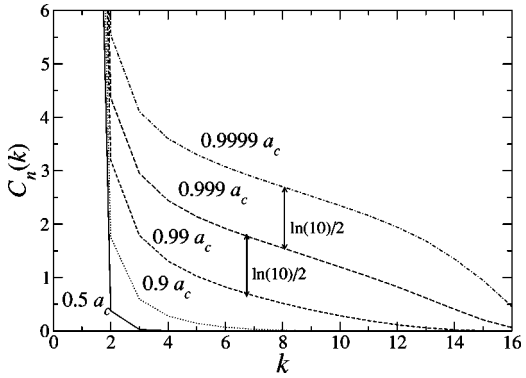

FIG. 11. Complexity profile for a long-range spin glass with $n=16$, for different values of a/a_c, averaged over 100 realizations of randomness.

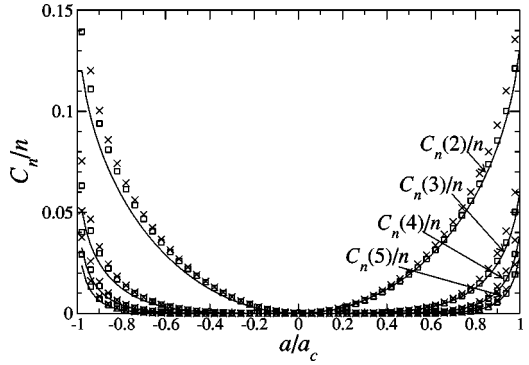

FIG. 12. Multiscale complexities for the mean-field spin glass, normalized by the number of spins, n, for $n=40$ (lines), $n=30$ (squares), and $n=20$ (crosses), averaged over multiple realizations of randomness.

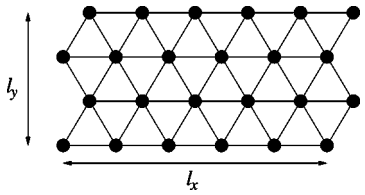

FIG. 13. Illustration of the orientation of the triangular lattice.

the behavior of the transition in the case of the spin glass and infinite-range magnet with uniform interactions. The scaling of $a_c \propto n^{-1/2}$ lies between that of the infinite-range ferromagnet ($a_c \propto n^{-1}$) and the antiferromagnet ($a_c = 1$) described in Sec. IV B.

Using these results, we explore the behavior of the multiscale complexities $C_n(j)$. Near a_c, we obtain a monotonically decaying positive curve, similar to that for the ferromagnetic mean-field magnet. For smaller values of a, the curve is shifted to lower values of $C_n(j)$, but does not become negative (see Fig. 11).

Interestingly, the curves of $C_n(k)$ for small k follow similar scaling behavior as those for ferromagnetic nearest-neighbor spin chains and lattices: when plotted as a function of a/a_c, $C_n(k)/n$ roughly collapses onto one curve for different n, as shown in Fig. 12. The exact values of the curves depend on the quenched variables, so that averaging over different realizations becomes necessary; however, the finite-size effects decrease with increasing n.

It is significant that the random and partly frustrated interactions do not lead to oscillations in the multiscale complexity. Ferromagnetic modes become dominant and trigger the transition before frustration has an impact. The study of spin glasses using replica symmetry breaking has previously found that the spin-glass order parameter has a degeneracy of order n in the ground state with spins having a macroscopic ordering in the direction of one of these low-energy states. Such macroscopic ordering is indeed similar to the ordering found in an infinite-range model and is qualitatively different from a frustrated infinite-range model which constrains the macroscopic state to a macroscopically degenerate subspace. Still, we note the different scaling between frustrated and unfrustrated interactions described above.

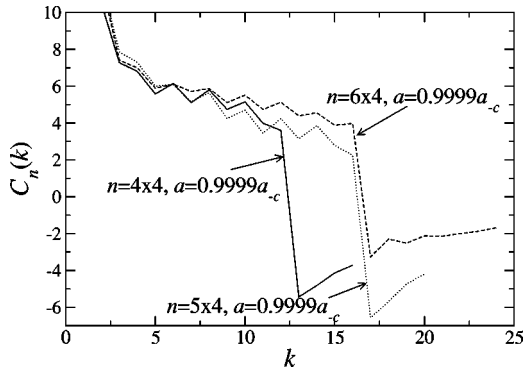

FIG. 14. Complexity profile for the triangular lattice near the antiferromagnetic transition, for different system sizes. One sees signs of both frustration and coherent behavior.

G. Triangular lattice

Our final example is a two-dimensional (2D) lattice with frustration in the antiferromagnetic state, the 2D triangular lattice. Again, we find two transitions points. In the ferromagnetic regime, the transition is $a = 1/6$ as expected for a lattice of coordination number 6. The complexity profile at the ferromagnetic transition is qualitatively similar to that of the square-lattice ferromagnet, and the multiscale complexity for small k is extensive. In the antiferromagnetic regime, the exact point of transition depends somewhat on the extent of the lattice in the x direction l_x (see Fig. 13): for example, it is $a_c = -1/3$ for $l_x = 3$, $-0.353\,553$ for $l_x = 4$, and $-0.350\,373$ for $l_x = 5$. For l_x that are compound numbers, the lowest absolute value of the transition for any of the divisors is the relevant one. The complexity profile near the transition (Fig. 14) now shows slight signs of frustration (small oscillations with k and negative values for $k \approx n$), but no large-amplitude oscillations as found for the infinite-range antiferromagnet. We interpret this as a sign of localized frustrations, consistent with a large ensemble of degenerate ground states, but with only local, rather than global, constraints.

VI. SUMMARY

Comparing the multiscale complexity profiles that were found in the preceding section, some intuitive and some

TABLE I. Comparison of qualitative features from from Secs. V A–V G.

Structure	Transition a_c	$C_n(k)$ extensive	Oscillations
Three-spin ferromagnet	$1/2$	N/A	no
Three-spin antiferromagnet	-1	N/A	yes
Infinite-range ferromagnet	$1/(n-1)$	no	no
Infinite-range antiferromagnet	-1	no	yes
Spin chain, n even	$1/2$	yes	no
Square lattice, L even	$1/4$	yes	no
Block matrices	varies	varies	varies
Infinite-range spin glass	$\propto 1/\sqrt{n}$	yes	no
Triangular ferromagnet	$1/6$	yes	no
Triangular antiferromagnet	$\approx -1/3$	no	weak

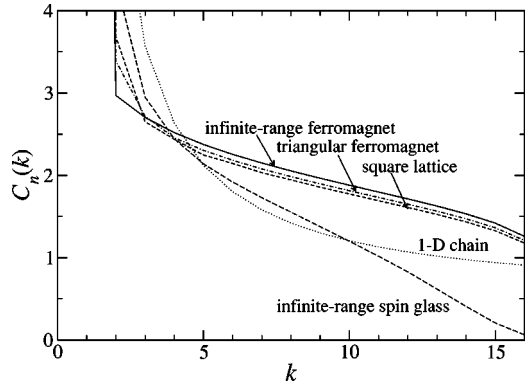

FIG. 15. Complexity profiles for different interactions that show monotonically decreasing $C_n(k)$, at the same ratio $a/a_c=0.999$, for $n=16$. The infinite-range ferromagnet, the square lattice, and the triangular lattice, yield remarkably similar curves.

rather surprising features emerge. The results are summarized in Table I and Fig. 15. All systems we considered show a transition from well-behaved (finite magnitude) spins to diverging-amplitude spins when the interaction between different spins overrides the self-interaction.

We find two different universal behaviors of the complexity profile: monotonic decrease with scale and oscillatory behavior. The former is a signature of systems with variables that are not frustrated. At the transition, spins become increasingly redundant because they are completely correlated (anticorrelated, in the case of an antiferromagnet) with each other. Near the critical point, complexities diverge logarithmically. Figure 15 shows a comparison between the curves near divergence (at $0.999a_c$, for $n=16$) for the interaction structures that show this behavior. The complexity profile can be interpreted as the cumulative spectrum of collective behaviors of the system. The independence of $C(k,\rho)$ with changes in ρ in all these cases implies that $D(k)=C(k+1)-C(k)$ is independent of ρ near the transition. Thus, the the collective behavior at $C(n)$ increases near the transition without changing the spectrum of excitations at all scales between 1 and n. One can see that the infinite-range ferromagnet, the square lattice, and the triangular lattice, yield very similar curves, whereas the infinite-range spin glass and the 1D chain show a quantitatively different decay. For the simple ferromagnetic systems (all except the spin glass) the value of $C_n(k)$ for large k appears to increase monotonically with spin connectivity.

Away from the transition, in the weak-coupling regime, one finds that $C_n(k)$ decays exponentially with k. This corresponds to fluctuations on small length scales, as one expects from systems in the disordered phase. In systems that have local interactions or disordered interactions (essentially, in all the cases we studied except for the mean-field ferromagnet and block matrices), multiscale complexities are approximately extensive—i.e., proportional to system size—for small k away from the transition. In the language of magnetic systems, this means that one observes a finite-size correlation length indicating small patches of correlated spins, each of which give a contribution to complexity. Finite-size effects (deviations from extensivity) are more pronounced for two-dimensional and infinite-range models as compared to the 1D spin chain, as is to be expected in higher-dimensional systems.

The complexities $C_n(k)$ for k of order 1 thus represent localized fluctuations, whereas nonvanishing $C_n(k)$ for k/n of order 1 represent the emergence of collective behaviors on the scale of the system as a whole and whose complexity is therefore not extensive. Since the multiscale complexity is a very general formalism, requiring only the joint probability distribution for input, it can thus be used to describe fluctuations and to identify phase transitions without explicitly choosing order parameters.

The second universal behavior, oscillations, is observed when a global constraint leads to redundancy: in the simplest case, for the long-range antiferromagnet, mutual repulsion enforces the constraint $\Sigma x=0$, implying that any one spin is determined if all others are known. We find that such constraints do not result from random interactions found in spin glasses; i.e., frustrated interactions do not necessarily result in frustrated variables. There exist enough interactions that are not frustrated to ensure collective behaviors of the ferromagnetic type. Oscillations do arise, however, for symmetric antiferromagnetic interactions, both between individual spins and between blocks of spins.

Finally, we note that the characterization that we have provided using the multiscale complexity is distinct from the usual characterization of the correlations in spatial systems using a correlation length. The multiscale complexity does not require a spatial structure. It identifies the aggregate size of fluctuations in terms of the number of participating spins regardless of the topology of spatial or nonspatial interactions. Thus it provides a more generally applicable characterization of the collective behavior in interacting systems.

ACKNOWLEDGMENT

We thank Mehran Kardar for important suggestions and fruitful discussion.

[1] C. E. Shannon, Bell Syst. Tech. J. **27**, 79 (1948). Published also in C. E. Shannon and W. Weaver, *The Mathematical Theory of Communication* (University of Illinois Press, Champaign, IL, 1963).

[2] T. S. Han and K. Kobayashi, *Mathematics of Information and Coding* (AMS, Providence, RI, 2002).

[3] C. M. Goldie and R. G. E. Pinch, *Communication Theory* (Cambridge University Press, Cambridge, U.K., 1991).

[4] F. Reif, *Fundamentals of Statistical and Thermal Physics* (McGraw-Hill, New York, 1965).

[5] R. Balian, *From Microphysics to Macrophysics* (Springer, Berlin 1982).

[6] Y. Bar-Yam, *Dynamics of Complex Systems* (Westwood Press, Boulder, CO, 1997); also for download at http://www.necsi.org/publications/dcs
[7] Y. Bar-Yam, Adv. Complex Syst. **7**, 47 (2004).
[8] S. Gheorghiu-Svirschevski and Y. Bar-Yam, Phys. Rev. E **70**, 066115 (2004).
[9] Y. Bar-Yam, Complexity **9**(4), 37 (2004).
[10] Y. Bar-Yam, Complexity **9**(6), 15 (2004).
[11] P.-M. Binder and J. A. Plazas, Phys. Rev. E **63**, 065203 (2001).
[12] J. P. Crutchfield and D. P. Feldman, Chaos **13** (1), 25 (2003).
[13] D. H. Hartnett, *Introduction to Statistical Methods*, 2nd ed. (Addison-Wesley, Reading, MA, 1975).
[14] I. Guttman, *Linear Models: An Introduction* (Wiley, New York, 1982).
[15] G. Parisi, *Statistical Field Theory* (Addison-Wesley, Redwood City, CA, 1988).
[16] L. D. Landau and E. M. Lifshitz, *Statistical Physics*, 3rd ed. (Pergamon, Oxford, 1980), Vol. 1.
[17] H. Simon, Proc. Am. Philos. Soc. **106**, 467 (1962).
[18] E. P. Wigner, Ann. Math. **67**, 325 (1958).
[19] K. H. Fischer and J. A. Hertz, *Spin Glasses* (Cambridge University Press, Cambridge, U.K., 1991).
[20] D. Chowdhury, *Spin Glasses and Other Frustrated Systems* (Princeton University Press, Princeton, NJ, 1996).